



# Histopathology of Chloroplast Ultrastructure and Inclusion Bodies in CMV-Infected Plant Tissues Using Electron Microscopic Examination and ImageJ Analysis

Magdy S Montasser<sup>1\*</sup> and Ayman E El-Sharkawey<sup>2</sup>

### Abstract

*Cucumber mosaic virus* (CMV) is an economically important virus that causes wide-spread diseases damaging crops worldwide. Two strains of the virus were detected using ELISA with specific antibodies, and isolated from Kuwait environment designated CMV-KU1 and CMV-KU2. The KU1 is a mild strain and is associated with a benign viral satellite RNA, while KU2 isolate, is a severe strain and lacking viral satellite RNA. Both strains were used in a comparative study to investigate the effects of CMV infection on the ultrastructure of chloroplasts and inclusion bodies in test plants of tomato (*Lycopersicon esculentum*) and squash (*Cucurbita pepo*). Transmission electron microscopy (TEM) was used to determine the extent of infection and damage caused by virus isolates on chloroplast structure, and cellular inclusions including plastoglobules, and starch granules. Chloroplasts, the photosynthetic apparatus of plants, in infected tissues were severely affected with KU2 strain that caused a reduction and damage of their main structure, number, size, and inclusion bodies compared to the benign strain of KU1 and healthy control plants. Electron micrographs of ultra-thin sections proved the presence of the viral nanoparticles. The formation of viral crystalline bodies, chloroplast damage and malformation due to the viral infection. As the infection progressed, chloroplasts were destroyed and grana were disorganized and scattered into the cytoplasm that causes reduction in chlorophyll contents in plant tissues. ImageJ freeware analysis were used to determine the extent of infection and host-virus interactions and damage caused by virus isolates.

### Keywords

Cucumber mosaic virus; CMV; Viral satellite rna; Nanoscopy; Transmission electron microscopy; TEM; Chloroplast; Plastoglobuli; Starch granules; ImageJ; Viral nanoparticles

## Introduction

*Cucumber mosaic virus* (CMV), first discovered by Doolittle in 1916 as the causative agent of a new infectious mosaic disease [1,2]. CMV, of the family *Bromoviridae*, genus *Cucumovirus* [3-6] is distributed worldwide and has a wide host range, infecting more than 1000 plant species [3,7-10]. In addition, it is considered to be the most

damaging plant virus among 24 field-grown vegetable crops in 28 regions of the world [11]. CMV is a 29 nm icosahedral. It is comprised of a positive-sense, single-stranded genome consisting of four species designated RNAs and a capsid composed of 180 copies of protein subunits [12-14]. The molecular weight of CMV is approximately  $5 \times 10^6$ , of which 18% is RNA and the remaining 82% is protein. The overall architecture of the CMV virus is best represented as a T<sub>4</sub> 3 icosahedron, [15] the RNA was packed tightly against the protein shell. CMV contains three genomic RNAs (RNAs 1, 2, & 3) and a subgenomic RNA 4 [12].

The symptoms of CMV in different plants occur as a result of complex interaction between the host plant and the virus [8,16]. In general, it induces mosaic (generic light-green/dark-green) symptoms. However, some CMV strains induce other symptoms, such as chlorosis, stunting, epinasty, necrotic lesions or filiformism [3,8]. In tomatoes, CMV causes stunting, fruit deformation, and poor fruit generation [1]. In addition to this, Vásquez and his associates have observed other unusual mixed disease symptoms on tomato plants including deformation, purple margins, inter-venial yellowing, downward and upward curling of the leaflets.

## Agriculture Industry in Kuwait

The State of Kuwait has a harsh climate, water scarcity and poor land resources and because of this agriculture is limited (Only about 1% of the total land in the country is employed for cultivation [17]. Kuwait mainly imports most of its food products to meet the increasing food demand. Recently, there have been increased efforts to enhance the agricultural production and much research has been undertaken in this field. Due to this, agriculture in Kuwait has doubled in the last 30-40 years. However, this is still diminutive for the national GDP [17,18]. Tomato is the main crop grown in Kuwait with a total production of almost 39,000 tons of fruit and economic value of about \$9.58 million. It is grown in 25% of total area under green house in Kuwait [18]. CMV was found to cause serious damage to plants in Kuwait, especially tomato, resulting in high economic losses in crop production over the last 10 years. Montasser and his colleagues in 2006 isolated three different strains of the CMV from different locations in Kuwait [1].

## Symptomatology

CMV disease symptoms were first observed as stunting or fern leaf syndrome, and lethal necrosis disease [19]. In addition, CMV viruses are also observed to cause yellow mosaic symptoms on leaf, leaf distortion, crinkle and stunting [5]. In few cases, expression of such specific symptoms has been mapped to specific amino acids in the capsid 1a or 2a proteins [8]. However, external symptoms can't be used as a sole criterion for confirming the disease, since masking of symptoms is observed during certain seasons in most of the infected plants [20]. It's very common in nature for a single plant to have mixed symptoms due to the infection by two or more viruses. Potyvirus, for example, can show mosaic systems that resemble CMV symptoms. Therefore, the complete separation of viruses is necessary for resistance studies.

In tomato, CMV causes systemic mosaic, necrosis, deformed fruit and poor fruit sets. Some CMV strains can produce symptoms of

\*Corresponding author: Magdy S, Montasser, Department of Biological, Faculty of Science, University of Kuwait, Kuwait PO Box 5969 Safat 13060, Kuwait, Tel: +96524985657, E-mail: magdy.montasser@ku.edu.kw

Received: May 04, 2017 Accepted: May 26, 2017 Published: May 29, 2017

severe shoestring leaves, chlorosis, and stunting in tomato. Two types of CMV disease patterns in tomato have been identified: The first is the shoestring or fern leaf syndrome, and the second pattern is the lethal tomato necrosis disease [19,21].

## Transmission Electron Microscopy (TEM)

Plant viruses can be detected and characterized by many methods. One of the oldest ways of detection is the electron microscopy that uses as a multi target assay [22]. Transmission electron microscopy (TEM) is used for detection and identification of viral nanoparticles and for investigation of ultrastructural alterations that occur during virus infection of plants [10]. Electron Microscopy studies have shown that CMV is spherical in shape [23,24] and can aggregate together to form crystals [25,26].

The plan and cross-sectional views are the two commonly used observation methods in the TEM analysis technique. The cross-sectional view is more favorable for obtaining micro-structural information since films grow coherently on the substrates and often present columnar crystals with preferred orientation [27]. Furthermore, staining with uranyl acetate has been a routine technique for staining the plant tissue. Negative staining of viruses and the following visualization by TEM can provide rapid and accurate results and they are sufficient for the identification of virus disease [10].

## Chloroplast Inclusion Bodies: Plastoglobules (“Osmophilic” Granules)

The occurrence of lipid granules in plastids. It was introduced the term ‘plastoglobuli’ to denote these osmiophilic granules. The size of plastoglobuli varies from 30 to 100 nm. They usually lack bounding membranes and are found scattered within the stroma. The amount present in any one chloroplast seems to depend on the rate of lipid synthesis. A densely staining droplet (about 30-100 nm) found, often in large numbers, in plastids of plant cells. Plastoglobuli consist of lipid pigment and are especially prominent in colored plastids (chromoplasts). Plastoglobuli occurs in chloroplasts but are masked by the green chlorophyll. When the chlorophyll breaks down as the leaves start to die due to the stress of viral infection, the pigmented plastoglobuli become apparent as the red or yellow ‘Fall’ colors [28-30]. During senescence stress of the cells of higher plants, there is also a marked increase in the accumulation of plastoglobuli. A similar increase in plastoglobuli during heterocyst formation in the blue-green algae *Chlorogloea* was reported [31]. Plastoglobuli contain carotenoids, plastoquinones, and a small amount of chlorophyll was reported in it [32].

## Starch granules

They are very common in chloroplasts, typically taking up 15% of the organelle's volume, though in some other plastids like amyloplasts, they can be big enough to distort the shape of the organelle. Starch granules are simply accumulations of starch in the stroma and are not bounded by a membrane. Starch granules appear and grow throughout the day, as the chloroplast synthesizes sugars, and are consumed at night to fuel respiration and continue sugar export into the phloem, though in mature chloroplasts, it is rare for a starch granule to be completely consumed or for a new granule to accumulate [33]. Starch granules vary in composition and location across different chloroplast lineages. In red algae, starch granules are found in the cytoplasm rather than in chloroplast. In  $C_4$  plants, mesophyll chloroplasts, which do not synthesize sugars, lack starch granules [28].

## Viral crystalline bodies

Crystalline inclusion bodies may be formed by both isometric and spherical viruses. The regular arrangement of the nanoparticles results in crystals that may be hexagonal or rounded in shape. The crystal of CMV have been extensively studied and showed to consist of closely stacked layers of nanoparticles arranged in parallel [34]. Crystal is produced by viruses belonging to many different virus groups including the cucumoviruses, the nepoviruses and the comoviruses [35-37]. The crystals may vary in size ranging from minute bodies that can only be seen in the electron microscope, to structures 15 to 20  $\mu\text{m}$  in diameter that is visible in the light microscope. ‘Empty’ virus crystals lacking virions located in a vacuole may appear as a neat hexagonal outline but more often appear as ‘empty’ circles. Such ‘empty’ crystals are diagnostic for CMV [38].

Image analysis of tissue sections using TEM RGB image profiling is a modern accepted technique. A new method of TEM RGB analysis, using the freeware ImageJ, is presented which can be applied to analyze area and value of different selections of tissue samples. We examined TEM micrographs of plant tissue samples indicated that the formation of crystalline bodies, chloroplast damage and malformation was due to the infection caused by viral infections.

## Materials and Methods

### Virus source

Leaves of tomato plants showing CMV like symptoms were collected as samples from different locations in Kuwait such as Wafra and Abdaly. CMV strains were detected using specific antibodies successfully produced in our laboratories applied in enzyme linked immunosorbent assay (ELISA) as described by Montasser 1999 [39]. Test plants of tomato (*Solanum Lycopersicum*) squash (*Curcubita Pepo*) sp. and tobacco (*Nicotiana tabacum* cv. Samson) were used in this study to confirm the infectivity of CMV.

### Mechanical inoculation of virus isolates and symptomatology

Tomato (Super Marmande, USA.), squash (New Eskandrany H1, Egypt) and tobacco were germinated under green house conditions, 16 hours light, 22-25°C [19,40]. One gram of frozen infected tissue of both tomato and squash plants was grounded using a sterile mortar and pestle with 9 ml of phosphate buffer (0.01 M potassium phosphate pH 7.2) 21 days post inoculation. The ground viral sap was mechanically inoculated onto the leaves of tomato, squash and tobacco using a cotton swab at the dicotyledonary stage of the plant growth. Healthy plants without any viral inoculations were also included as control treatments. Before inoculation, plant seedlings were pre-dusted with 600- mesh carborundum powder to allow for better viral transmission into the leaves. Following inoculation, the plants were rinsed with distilled water immediately [19,39].

### Maintenance of virus isolates

Test plants were grown in pots using a suitable potting mix both in green house and in a growth chamber under controlled condition (16 hours light, temperature range 22-25°C). The inoculated plants showed symptoms between 8-20 days [19]. Infected plant leaves were collected for electron microscopy studies and for molecular analysis for microarray studies, tomato samples were collected 20 days post inoculation.

## Ultra- Thin Sectioning of Plant Tissues Using TEM Analysis

### Sample preparation and fixation

For sample preparation infected tomato and squash tissue parts such as STEM, leaf, and roots as well as healthy tissues were collected. Tissue samples were sliced and fixed in glutaraldehyde 3% and in phosphate buffer solution with the range between pH=7.2-7.4, these samples were kept at room temperature for one to two hours before placing them in the refrigerator overnight.

Fixation was followed by three washes with phosphate buffer solution for ten minutes each time. Samples were post-fixed in a solution containing 2% osmium tetroxide in phosphate buffer solution for two hours at room temperature on a slow-speed rotator (INFIL- Tissue Rotator). This step was repeated thrice as it is described above. Dehydration of the fixed samples were carried out using different concentrations of alcohol ranging from 50-100% and propylene oxide in a Leica Automatic Tissue Processor (REICHEART- LYNX). Following this, infiltration was done by soaking samples in different ratios of propylene oxide: super resin mixture. Both dehydration and infiltration steps were carried out at a temperature of around 20°C.

### Trimming and ultramicrotomy

Practical 1 µm of semi- thin sections were cut with a **glass knife** using Leica Ultramicrotomy and placed on microscopic glass slide. After that, they were stained with toluidene 1% blue and examined under a light microscope to locate the desired area. Ultra- thin sections about 70-80 nm were made using a **diamond knife**, and transferred onto 150 mesh copper grid. The loaded grids were **stained** first with uranyl acetate (12 min. at 25°C) followed by lead citrate (6 min. at 25°C). Finally, the stained sections were examined by transmission electron microscope TEM (JEOL's JEM- 1200 EX II) operated at an accelerating voltage of 80 kV, at Nanoscopy Science Center (NSC) – Kuwait University, Kuwait.

### Computational image analysis

Using TEM with imageJ analysis and statistical Origin Pro 2016 program for quantification of the infection influences on chloroplast structure and contents of lipid deposits in plastoglobuli, starch grains, nanoparticle size, size distribution and profile surface area [41,42]. For image analysis, the freeware ImageJ v 1.51A as well as the Color Histogram, distribution, analyze nanoparticles size and 3d plug-in, both downloaded from the NIH website [41] were used.

To calculate the FWHM of a Gaussian peak following relation should be considered.

$$FWHM = 2\sigma \cong 2.35\sigma \quad (*)$$

Therefore, the deviation from the mean value at FWHM will be somewhat larger than the regular  $\sigma$  obtained from the following Gaussian equation

$$f(x) = y_o + \frac{A}{w\sqrt{\pi/2}} \exp\left(-\frac{2(x-x_o)^2}{w^2}\right) \quad (**)$$

Where  $y_o$  is baseline offset,  $A$  is the total area under the curve from the baseline,  $x_o$  is the mean value of the Gaussian peak (center of the peak or  $x_c$ ), and  $w/2$  is the standard deviation  $\sigma$  (Figure 18D).

## Results

### Disease incidence and symptomatology

CMV-KU2 isolate caused serious damage to tomato and squash test plants causing severe stunting and growth reduction (Figure 1, 2A and 2B) 20 days post inoculation. Squash plants infected with CMV-KU2 produced no flowers (aborted flower buds) compared to healthy control (Figure 1C). Squash plants infected with CMV-KU1 showed mild stunting and chlorotic local lesions on the dicotyledonary leaves (Figure 3). Both viral strains were detected by using ELISA test and specific antibodies successfully produced in our laboratory. Squash plants produced more severe mosaic symptoms compared to tomato plants. Squash leaves showed mosaic, yellowing and curling symptoms (Figure 2). Infected plants with CMV-KU1 flowered in earlier stage producing smaller flowers *vis.* CMV-KU2 showed severe

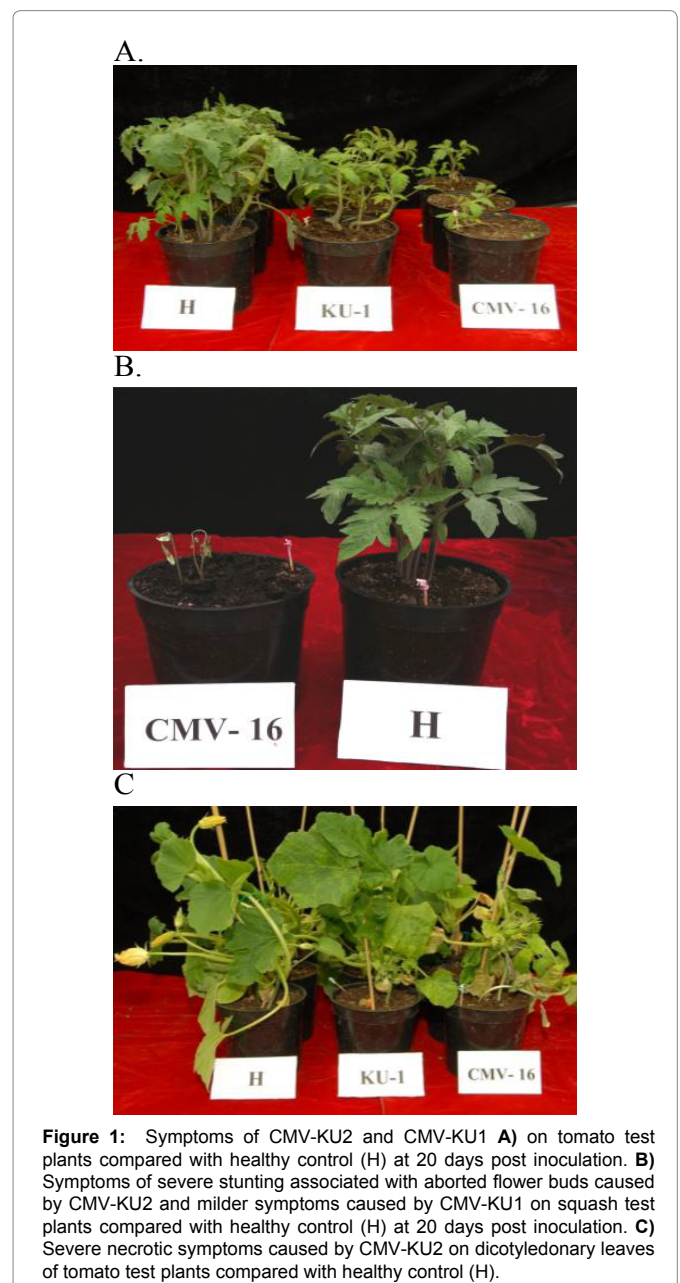


**Figure 1:** Symptoms of CMV-KU2 and CMV-KU1 **A)** on tomato test plants compared with healthy control (H) at 20 days post inoculation. **B)** Symptoms of severe stunting associated with aborted flower buds caused by CMV-KU2 and milder symptoms caused by CMV-KU1 on squash test plants compared with healthy control (H) at 20 days post inoculation. **C)** Severe necrotic symptoms caused by CMV-KU2 on dicotyledonary leaves of tomato test plants compared with healthy control (H).

mosaic symptoms compared to CMV-KU1 and control (Figure 2)

### Nanoscopy analysis using TEM

**Ultra-thin sections:** TEM micrographs of healthy and infected intracellular structure are shown in Figures 3-5. A close-up view of the chloroplast structures showing double membranes, grana, thylakoids, stroma and plastoglobuli (Figure 4C) while an overview of the infected tissues showing the effect of CMV-KU2 infection on chloroplasts compared to healthy squash are shown in Figures 6 and 7.

A closer examination of these tissues revealed that characteristic morphological nature of CMV strains in the infected tissue in contrast to healthy samples (Figures 6 and 7). Changes in the chloroplast structure due to infection are presented in Figures 6B and 7B compared to the healthy chloroplast. Ultrathin sections showed the presence of CMV nanoparticles as small regular spherical bodies that contain homogenous densely stained genetic materials (Figure 7) (Magnification of 40000x for the virus nanoparticles) (Figure 8). The severity of CMV-KU2 showed the disintegration of chloroplasts with broken grana scattered in the cytoplasm and virus nanoparticles are aggregated in large numbers around the broken-down chloroplasts (Figure 7B).

Virus nanoparticles are aggregated together as shown in Figure 9, forming crystalline bodies in CMV-KU1 infected tissues (Figure 10). No crystalline bodies were found in CMV-KU2 infected tissues, while the virus nanoparticles are packed in geometric rows.

In transverse thin sections of the infected tissue, most abundant virus nanoparticles were observed in CMV-KU2 infected tissues. Symptoms caused by CMV-KU2 were more severe than CMV-KU1 infected plants. Similarly, CMV-KU2 damaged the chloroplast and was more severe than CMV-KU1 (Figure 11) that clearly showing starch grains.

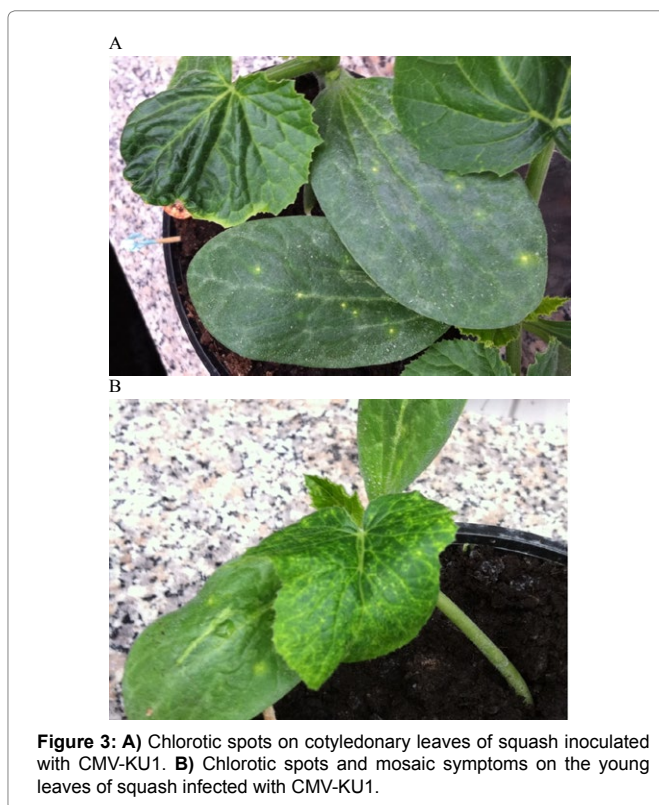


**Figure 3:** A) Chlorotic spots on cotyledonary leaves of squash inoculated with CMV-KU1. B) Chlorotic spots and mosaic symptoms on the young leaves of squash infected with CMV-KU1.

**Effects of CMV strains infection on the ultra-structure of chloroplasts:** The morphological appearance of the chloroplast was totally damaged and major alteration took place in the chloroplast ultra-structure that were observed in the aggressive stage of infection. As the infection progressed, the chloroplast double membranes were destroyed and the grana were smashed, disorganized and scattered in the cytoplasm of the infected tissue (Figures 12 and 13).

**Computational analysis of tem micrographs using imagej:** Using Freeware ImageJ to analyzed TEM images for chloroplast structure (Figure 14A-D), lipid deposits in Plastoglobuli (Figure 15A-Dd), and starch grains (Figure 16A-D), crystalline bodies of aggregated CMV nanoparticles (Figure 17A and B). TEM images Analysis for aggregate CMV nanoparticles size and distribution and standard deviation analysis (Figure 18A-D) Morphology of mitochondria and its surface profile (Figure 19A-E).

The relationship between a standard deviation ( $\sigma$ ) and a full width at half maximum (FWHM) for a Gaussian peak. Note that the magnitude of the deviation from the mean value at FWHM is slightly larger than the deviation at  $\sim 60\%$  of the peak height i.e.,  $\sigma$ . (Figure 18D)

Average NP size (xc)	= 38.53 nm
W	= 87.06 nm
Now standard deviation ( $\sigma$ )	= $W/2 = 43.53$ nm
Average NP size with error	= $Xc \pm \sigma = 28.53 \pm 43.53$ nm

### Discussion

In this study, two different strains of CMV designated CMV-KU1 and -KU2 (US patent No. US 8138390 B2) [43]. Were used to explore the pathogenic effects of the severe strain of KU2 compared to the

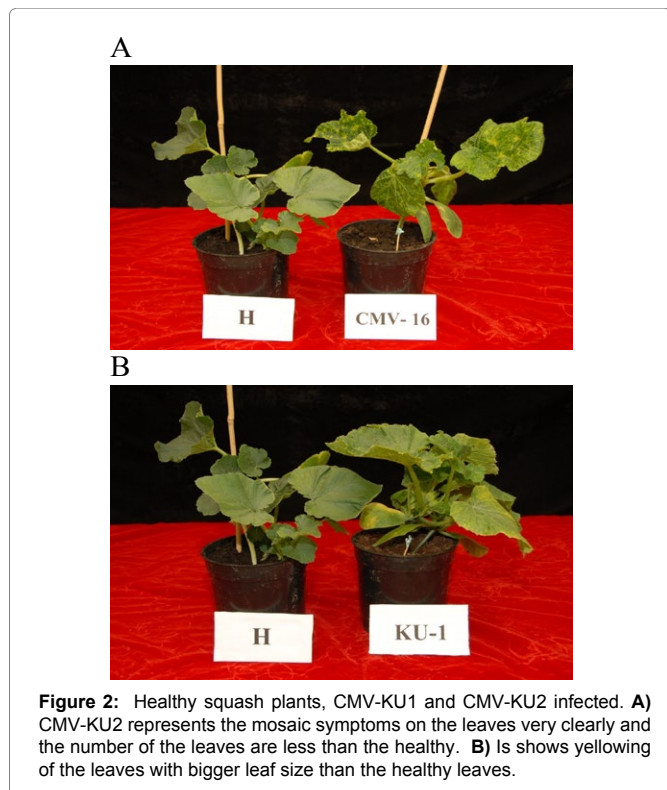


**Figure 2:** Healthy squash plants, CMV-KU1 and CMV-KU2 infected. A) CMV-KU2 represents the mosaic symptoms on the leaves very clearly and the number of the leaves are less than the healthy. B) Is shows yellowing of the leaves with bigger leaf size than the healthy leaves.

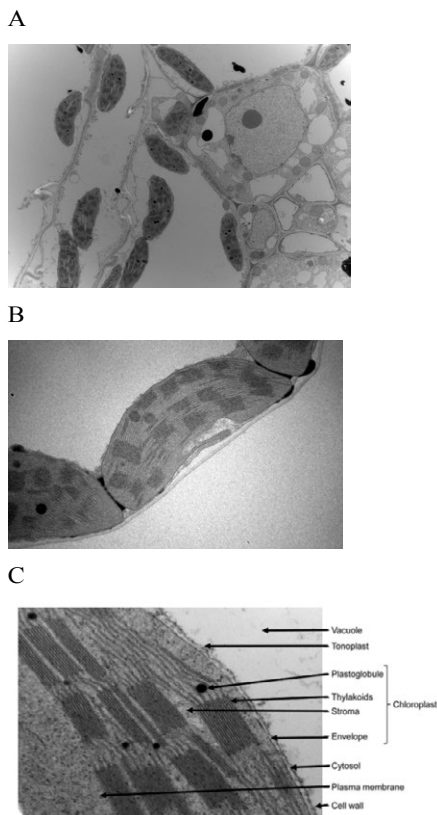


**Figure 4:** A) Normal healthy view of squash leaf tissue. B) Healthy chloroplast intra-structure of tomato cotyledons leaf. C) Chloroplast Structure.

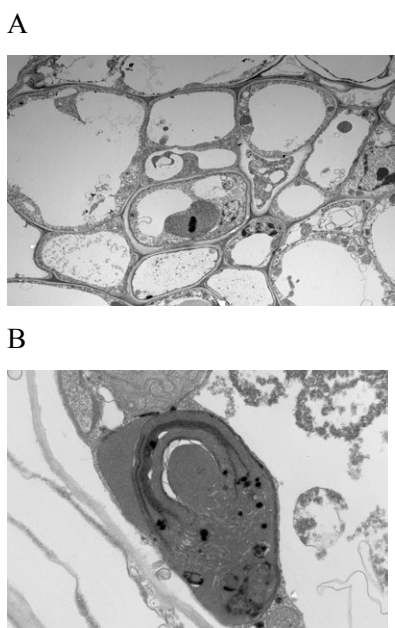


**Figure 5:** A) Overview of tomato infected root tissue showing that may indicate the viral infection spread all over the tissue, B) Infected chloroplast with CMV-KU2 in tomato leaf. The infection led to the malformation in the outer and inner structure of the chloroplast. The photo shows virus aggregation like nanoparticles spread in the tissue. Chloroplast and CMV-KU2.

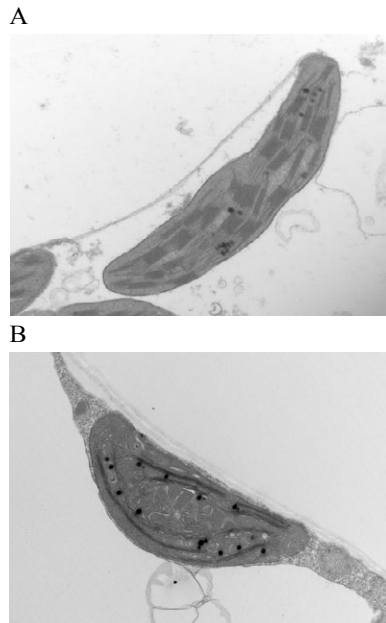


**Figure 6:** A) Comparison between two chloroplasts in healthy squash cotyledonary leaf. B) Anatomical deviations: intra-cellular structures showing complete destructions in grana and thylakoids, and malformations in a chloroplast.

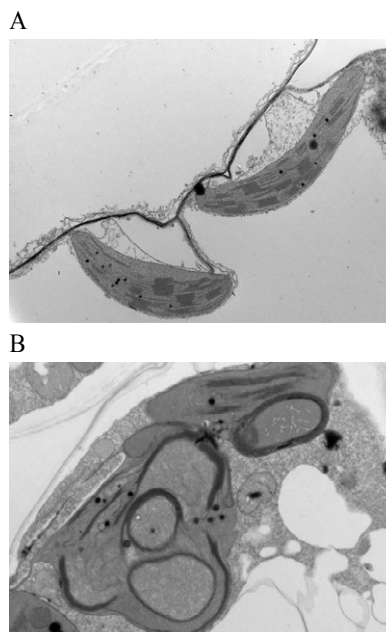


**Figure 7:** TEM micrographs of healthy and infected tomato showing damaged chloroplasts. A) Chloroplasts in healthy tomato cotyledonary leaf. B) Malformation and total damage in a chloroplast of tomato leaf infected with CMV-KU2 showing presence of virus nanoparticles surrounding the chloroplast.

benign strain of KU1 and healthy control. Transmission electron microscopy (TEM) was used for detection and identification of viral nanoparticles and for investigation of ultrastructural alterations that occur during virus infection of plants [10]. Nanoscopy studies have shown that CMV is spherical in shape [23,24] and can aggregate

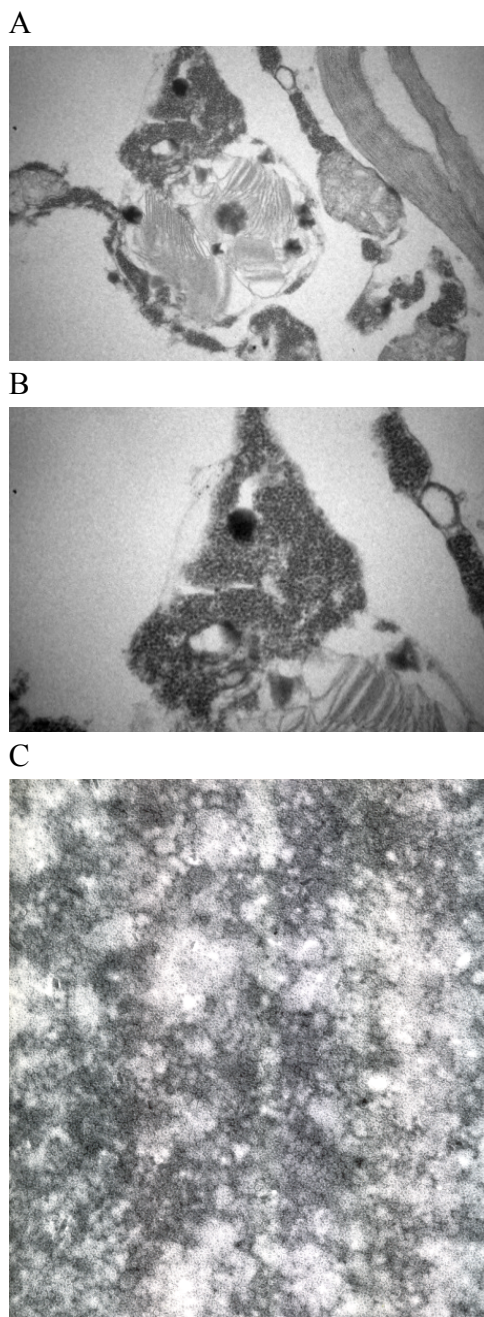


**Figure 8:** A) Broken chloroplasts in CMV-KU2 infected tissues showing scattered grana and thylakoids, virus nanoparticles aggregated in large numbers around the ruptured chloroplast. B) Close up from A. C) Higher magnification of purified CMV viral nanoparticles that are spherical with dark highly dense genetic material in the center. Purified viral nanoparticles from infected squash leaves.

together to form crystals [26]. Difficulties in sample preparation also limit the application of cross-sectional TEM observation [27]. Such preparations are known to be time and labor consuming and it may take several days to obtain results. For these reasons, TEM is used rarely for diagnosing virus disease in plants [27]. The plan and cross-sectional views are the two commonly used observation methods in the TEM analysis technique. The cross-sectional view is more

favorable for obtaining micro-structural information since films grow coherently on the substrates and often present columnar crystals with preferred orientation [27].

#### Ultra-thin sections

Electron micrographs of healthy and infected intracellular structure tissues are shown in Figures 4A and B. Micrographs of healthy samples are shown in Figure 4C and 4A shows an overview of the chloroplast structures double membranes, grana, thylakoids, stroma and lipid globules are shown in Figure 4C and 4A shows an overview of a healthy tissue while (Figure 5A) represents an overview of the infected tissues. Figure 5B shows the effect of CMV-KU2 infection in tomato chloroplasts.

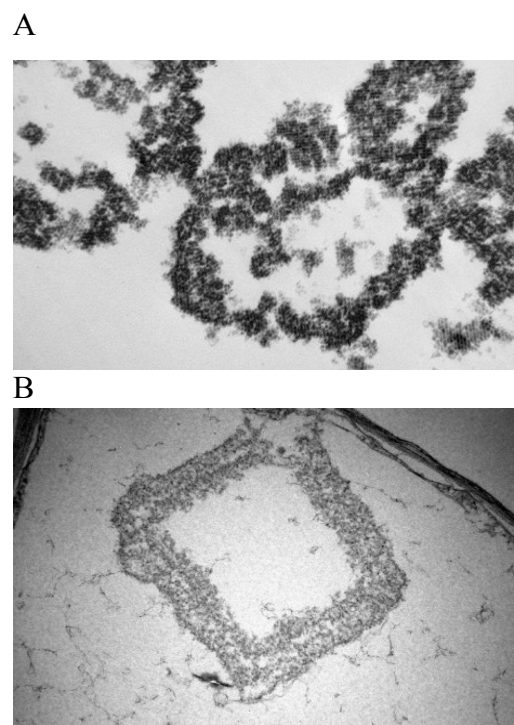


**Figure 9:** A) CMV Viral nanoparticles appear in geometric rows in preparations to form crystalline bodies. B) CMV Aggregation forming inclusion crystals in tomato infected leaf.

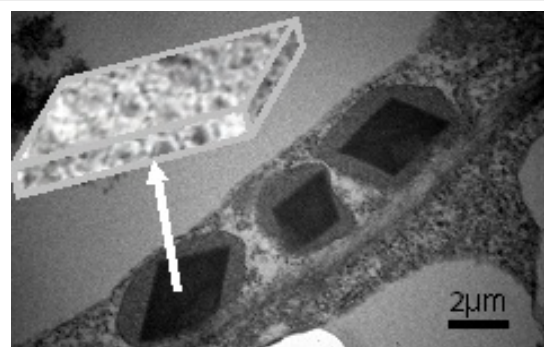
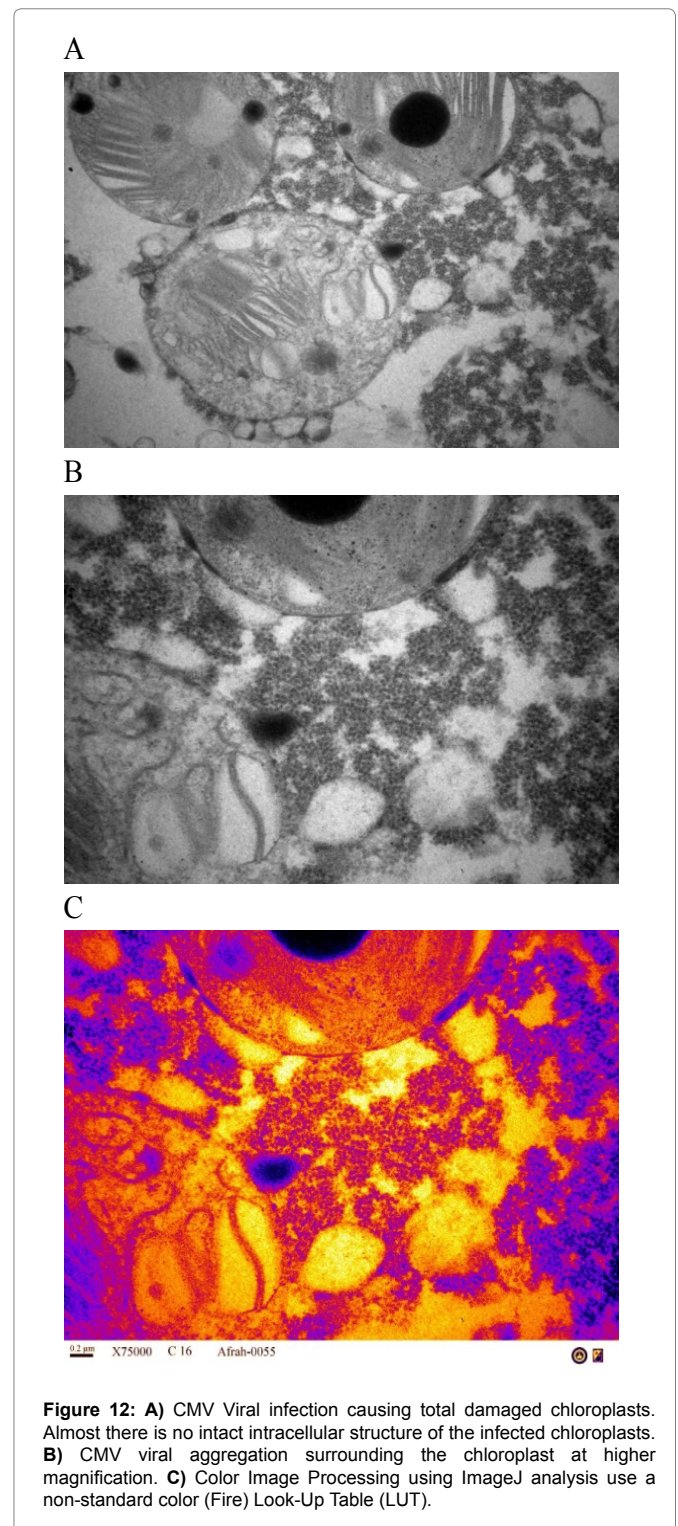
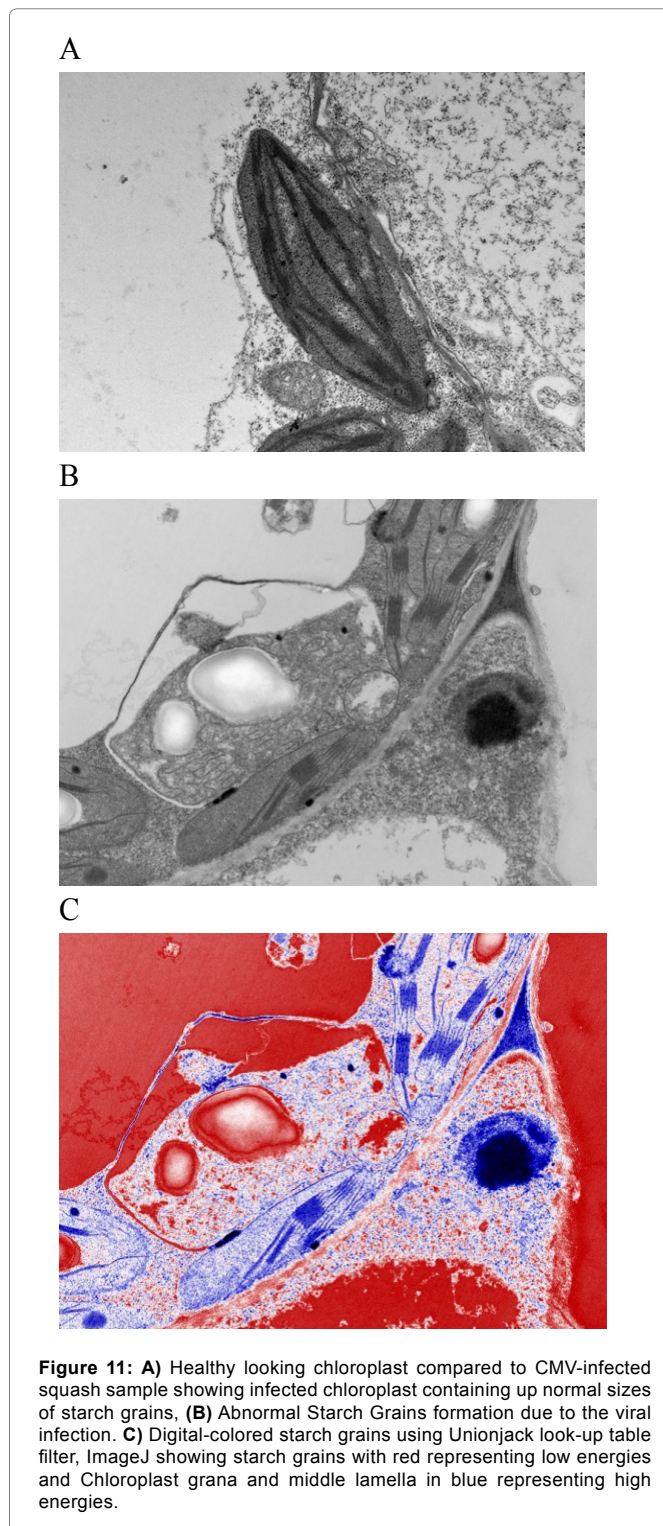


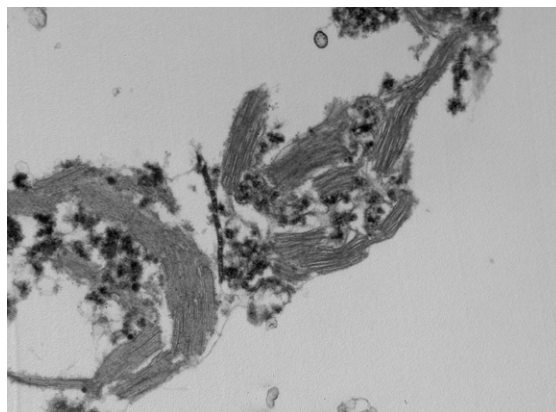
**Figure 10:** Viral inclusion crystalline bodies in tomato cells infected with CMV KU1 appear as heavy dense stained crystals, 3D diagrammatic presentation of virus inclusion crystal showing rows of spherical nanoparticles stacked in the component layers of crystals



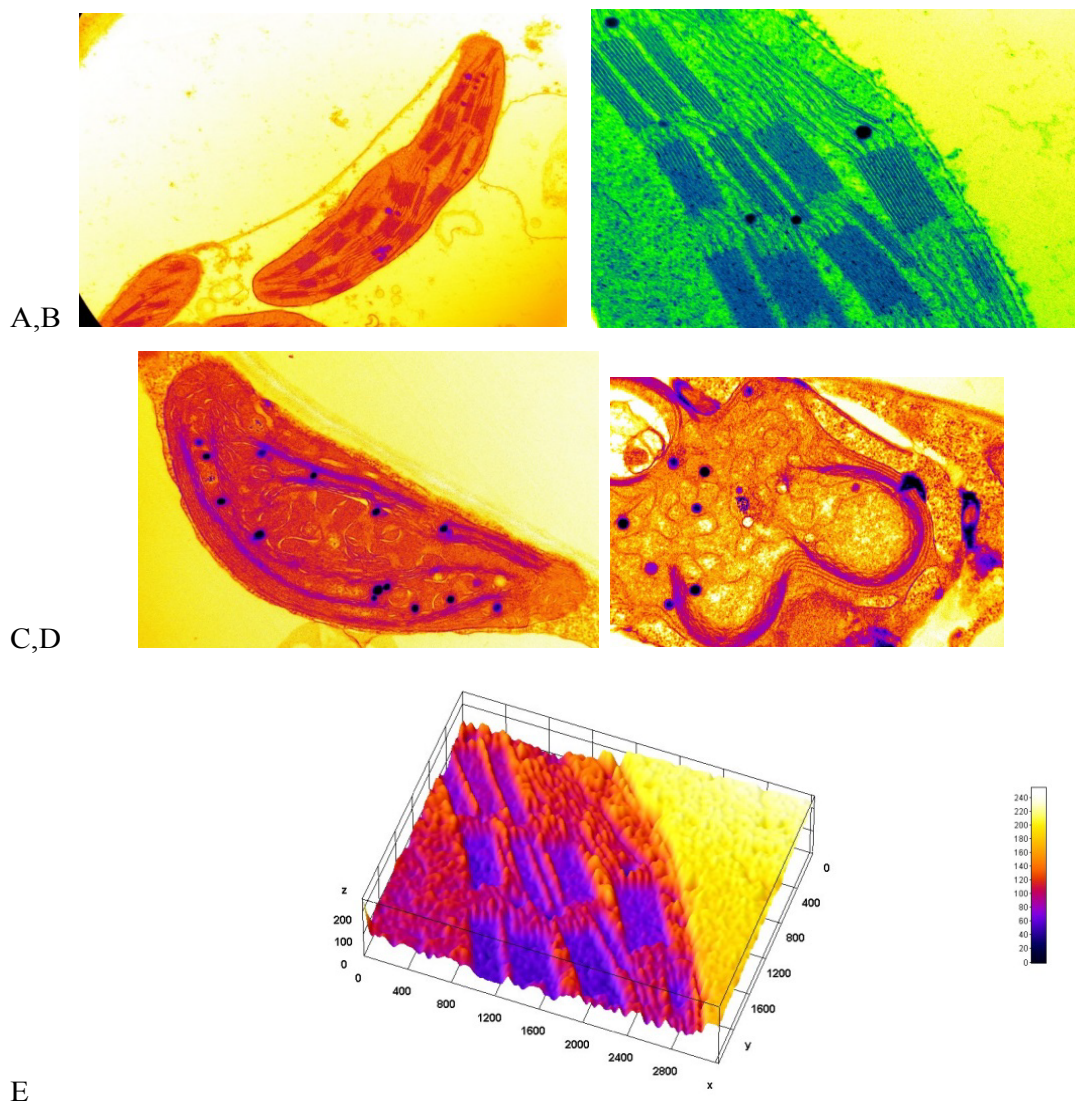
A closer examination of these tissues revealed the characteristic morphological nature of CMV strains in the infected tissue in contrast to healthy samples (Figures 6 and 7). Changes in the chloroplast structure due to infection are presented in (Figures 6B and 7A) compared with healthy chloroplast. Ultrathin sections showed the presence of CMV nanoparticles as small regular spherical bodies that contain a homogenous densely stained genetic materials in Figure

8 (magnification of 40000x for the virus nanoparticles) (Figure 8B). The severity of CMV-KU2 has been showed by the disintegration of chloroplasts with broken grana scattered in the cytoplasm and virus nanoparticles that are aggregated in large numbers around the broken-down chloroplasts (Figure 7B).

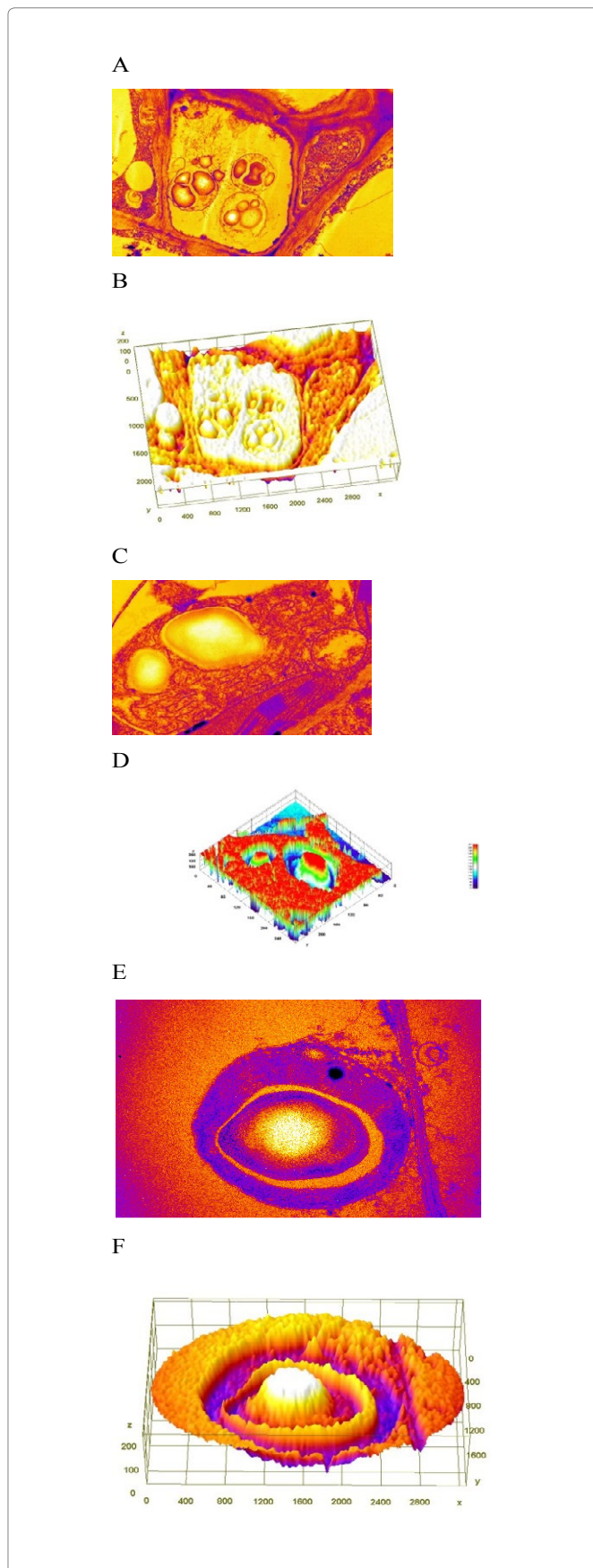
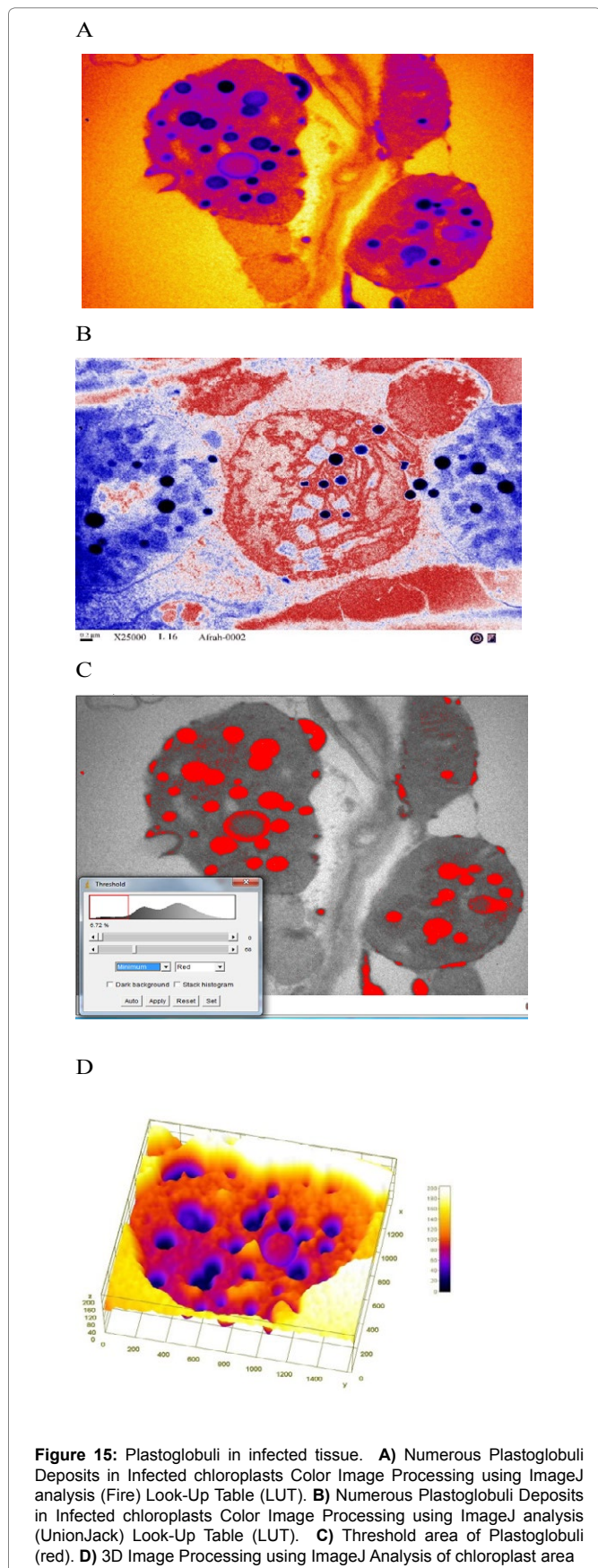
According to the scale bar (0.2  $\mu\text{m}$ ) the average of about 100



**Figure 13:** Destroyed chloroplasts due to CMV-KU2 infection. CMV particle aggregation in broken thylakoids.



**Figure 14:** A, B) Color Image Processing using ImageJ analysis (Fire filter) Look Up Table (LUT) for Healthy chloroplast compared to C, D) infected chloroplast. E) 3D Image Processing using ImageJ analysis of B image.



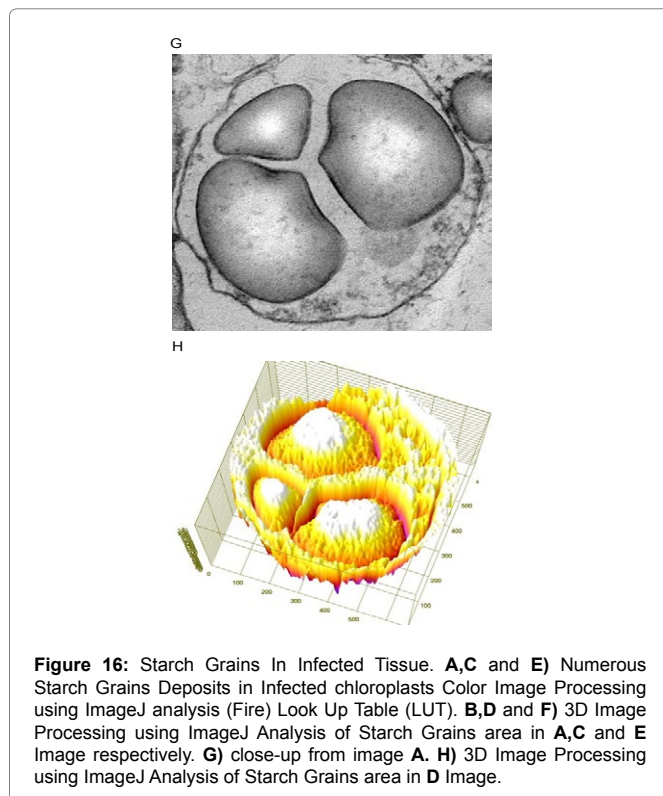


**Figure 16:** Starch Grains In Infected Tissue. **A,C** and **E**) Numerous Starch Grains Deposits in Infected chloroplasts Color Image Processing using ImageJ analysis (Fire) Look Up Table (LUT). **B,D** and **F**) 3D Image Processing using ImageJ Analysis of Starch Grains area in **A,C** and **E** Image respectively. **G**) close-up from image **A**. **H**) 3D Image Processing using ImageJ Analysis of Starch Grains area in **D** Image.

CMV samples was calculated manually and resulted in viral diameter of 26 nm-29 nm. CMV nanoparticles are packed to form crystalline bodies in CMV-KU1 infected tissues as shown in (Figure 9) were no crystalline bodies found in CMV-KU2 infected tissues. In transverse thin sections of the infected tissue most accumulation of the virus nanoparticles appeared in CMV-KU2 infected tissues (the affectively on the intracellular and the damaged caused on chloroplast structure is more) and its severity is more than in CMV-KU1 infected tissues.

Electron micrographs of CMV-infected tissues in ultra-thin sections were successfully tested and proved to be present in the infected intracellular plant tissues. The effects of the virus on the plant cellular organelles were detected. The ultra-structure of CMV infected cells showed spherical nanoparticles of the virus.

Our observation is consistent with those of Honda and Matsui [44]. The spherical CMV nanoparticles were observed in different locations in plant tissues [19]. Our results were agreeable with the viral particle sizes published, that found CMV nanoparticles are isomeric, 28-29 nm in size with a central core [45]. CMV nanoparticles were able to aggregate in geometric lines in tobacco plant [44] or aggregate to form crystalline bodies in lily [26]. In general, the various morphological arrangements of CMV were observed clearly in tested diseased plant tissues.

The present study showed some alterations in ultra-structure of chloroplasts in infected tomato and squash tissues compared with healthy plants. Similar effects of CMV on plant chloroplast grana and intracellular composition were mentioned by Shintaku et al. [46] on tobacco plants as well as others [19,44]. The concentration of virus varied in different plant tissues [26]. Another plant virus in Kuwait has induced the same effect, such as tomato yellow leaf curl bigemini

virus (TYLCV) on the same tomato host [43].

### The effect of viral infection on chloroplasts in tested plant tissues

The morphological appearance of the chloroplast as well becomes more circular and major alternation in the chloroplast ultra-structure at aggressive stage of infection. As the infection achieved, the chloroplast is completely destroyed and the grana were disorganized and scattered in the cytoplasm of the infected tissue (Figures 12-13). Comparisons between the healthy and the infected tissues (Figures 6 and 9) are made and a reduction in the size and number of grana causing a great loss in the chloroplast structures and increased in the multiplication of viral nanoparticles.

All over the infected tissues (Figures 5-13), the viral infection showed a reduction of chloroplast numbers and size [47]. The complete distortion of the chloroplast component and thylakoid

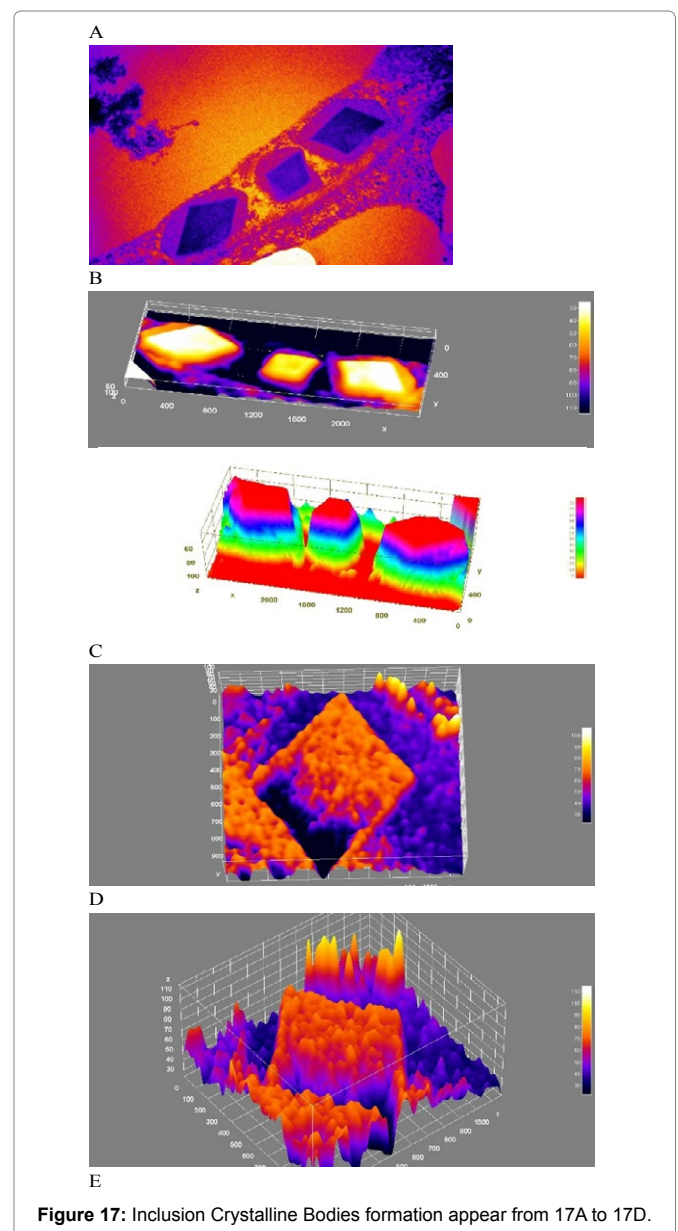


**Figure 17:** Inclusion Crystalline Bodies formation appear from 17A to 17D.

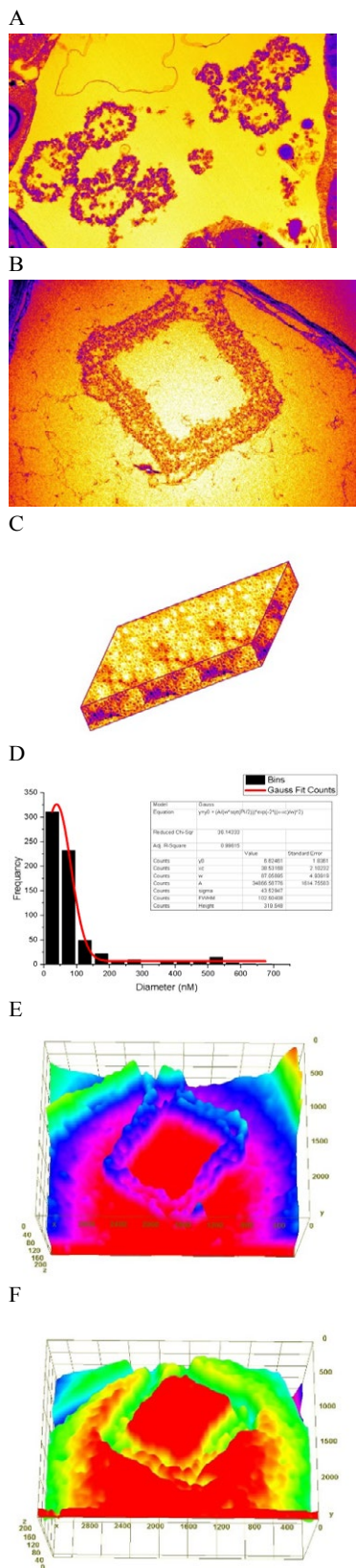


**Figure 18:** Aggregate CMV nanoparticles Size and distribution and standard deviation analysis:- Gaussian distribution.

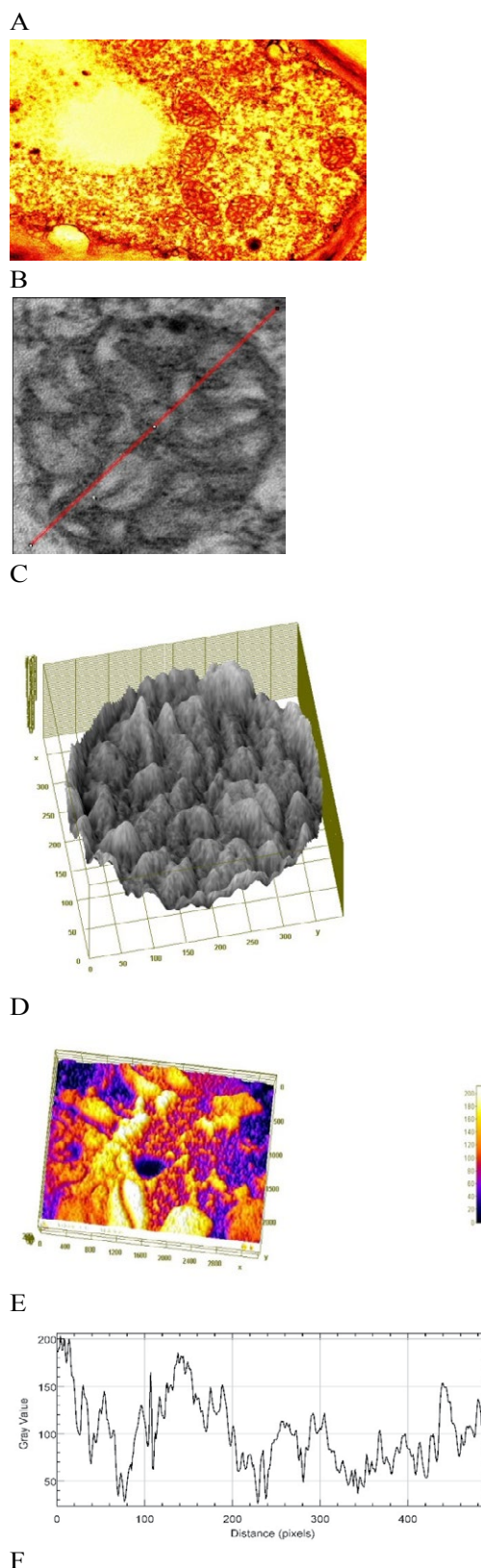


**Figure 19:** Mitochondrial Morphology and surface plot using ImageJ Freeware analysis from Figure (19A-19E).

damage in grana causes a reduction in chlorophyll concentrations in tissues.

Examination of ultra-thin sections of diseased plant parts using Transmission Electron Microscope has become a standard tool in establishing the presence of CMV. Further evidence can be obtained by ELISA [40], PCR, Gene Sequencing analysis, and Microarray technology. The physical properties (thermal inactivation point, dilution-end point and longevity *in vitro*) of CMV in Kuwait have been reported by [1].

### Computational analysis using ImageJ

ImageJ supports standard image processing functions such as logical and arithmetical operations between images, contrast manipulation, convolution, Fourier analysis, sharpening, smoothing, edge detection, and median filtering [42]. In this study, we detected and characterized the causal agent nanoparticles of cucumber mosaic disease on tomato and squash plants using TEM micrograph and ImageJ statistical Origin pro-2016 software Image analysis of tissue sections using TEM RGB image profiling is a modern accepted technique. A new method of TEM RGB analysis, using the freeware ImageJ that applied to analyze area and value of different selections of tissue samples. We examined TEM micrographs of plant tissue samples indicated that the formation of crystalline bodies, chloroplast damage and malformation was due to the infection caused by viral infections [41,42].

### Acknowledgement

This research work was supported and funded by the University of Kuwait, College of Graduate Studies, the Research Administration project No. YS07/10 & SL01/13 and Nanoscopy Scientific Center (NSC) at Kuwait University, Kuwait

### References

1. Montasser MS, Ali NY, Al Hamar B (2006b) Occurrence of three strains of *cucumber mosaic virus* affecting tomato in Kuwait. *Plant Pathol J* 22: 51-62.
2. Palukaitis P, Roossinck MJ, Dietzgen RG, Francki R (1992) Cucumber mosaic virus. *Advances in virus research* 41: 281.
3. Choi SK, Choi JK, Ryu KH (2003) Involvement of RNA2 for systemic infection of *cucumber mosaic virus* isolated from lily on zucchini squash. *Virus research* 97: 1-6.
4. De Wispelaere M, Rao A (2009) Production of *cucumber mosaic virus* RNA5 and its role in recombination. *Virology* 384: 179-191.
5. Shaban M, Al-Awadhi H, Hadidi A (2002) Identification of luteovirus nucleotide sequences in mild yellow-edge diseased strawberry plants. *Plant Pathol J* 18: 1-5.
6. Yamaguchi N, Seshimo Y, Yoshimoto E, Ahn HI, Ryu KH, et al. (2005) Genetic mapping of the compatibility between a lily isolate of *cucumber mosaic virus* and a satellite RNA. *J Gen Virol* 86: 2359-2369.
7. Montasser MS, Al-Own FD, Haneif AM, Afzal M (2012) Effect of tomato yellow leaf curl bigeminivirus (TYLCV) infection on tomato cell ultrastructure and physiology. *Can J Plant Pathol* 34: 114-125.
8. Du Z, Chen F, Zhao Z, Liao Q, Palukaitis P, et al. (2008) The 2b protein and the C-terminus of the 2a protein of *cucumber mosaic virus* subgroup I strains both play a role in viral RNA accumulation and induction of symptoms. *Virology* 380: 363-370.
9. Jacquemond M, Amselem J, Tepfer M (1988) A gene coding for a monomeric form of *cucumber mosaic virus* satellite RNA confers tolerance to CMV. *Mol Plant-Microbe Interact* 1: 311-316.
10. Zechmann B, Zellnig G (2009) Rapid diagnosis of plant virus diseases by transmission electron microscopy. *J Virol Methods* 162: 163-169.
11. Kaper J (1993) Satellite-mediated symptom modulation: an emerging technology for the biological control of viral crop disease. *Microb Releases* 2: 1-9.
12. Ding SW, Anderson BJ, Haase HR, Symons RH (1994) New overlapping gene encoded by the *cucumber mosaic virus* genome. *Virology* 198: 593-601.
13. Sgro JY, Jacrot B, Chroboczek J (1986) Identification of regions of brome mosaic virus coat protein chemically cross-linked in situ to viral RNA. *Eur J Biochem* 154: 69-76.
14. Smith TJ, Chase E, Schmidt T, Perry KL (2000) The structure of *cucumber mosaic virus* and comparison to cowpea chlorotic mottle virus. *J Virol* 74: 7578-7586.
15. Smith C, Tousignant M, Geletka L, Kaper J (1992) Competition between *cucumber mosaic virus* satellite RNAs in tomato seedlings and protoplasts: a model for satellite-mediated control of tomato necrosis. *Plant disease* 76: 1270-1274.
16. Shang J, Xi DH, Huang QR, Xu MY, Yuan S, et al. (2009) Effect of two satellite RNAs on *Nicotiana glutinosa* infected with *cucumber mosaic virus* (CMV). *Physiol Mol Plant Pathol* 74: 184-190.
17. Alomirah HF, Al-Zenki SF, Sawaya WN, Jabsheh F, Husain AJ, et al. (2010) Assessment of the food control system in the state of Kuwait. *Food control* 21: 496-504.
18. Al-Nasser AY, Bhat N (1998) Protected agriculture in the state of Kuwait. 15-18. Proceedings of the Workshop on Protected Agriculture in the Arabian Peninsula.
19. Montasser MS, Bader AH, Bhardwai RG (2006a) Biological control of a severe viral strain using a benign viral satellite RNA associated with cucumber mosaic virus. *Plant Pathol J* 22: 131-138.
20. Siju S, Madhubala R, Bhat A (2007) Sodium sulphite enhances RNA isolation and sensitivity of *cucumber mosaic virus* detection by RT-PCR in black pepper. *Journal of virological methods* 141: 107-110.
21. McGarvey P, Montasser M, Kaper J (1994) Transgenic tomato plants expressing satellite RNA are tolerant to some strains of cucumber mosaic virus. *J Am Soc Hortic Sci* 119: 642-647.
22. Boonham N, Walsh K, Smith P, Madagan K, Graham I, et al. (2003) Detection of potato viruses using microarray technology: towards a generic method for plant viral disease diagnosis. *J Virol Methods* 108: 181-187.
23. Kumar S, Raj S, Sharma A, Varma H (2005) Genetic transformation and development of *cucumber mosaic virus* resistant transgenic plants of *Chrysanthemum morifolium* cv. Kundan. *Scientia horticultrae* 134: 40-45.
24. Suehiro N, Matsuda K, Okuda S, Natsuaki T (2005) A simplified method for obtaining plant viral RNA for RT-PCR. *J Virol Methods* 125: 67-73.
25. Hatta T, Francki R (1981) Cytopathic structures associated with tonoplasts of plant cells infected with cucumber mosaic and tomato aspermy viruses. *J Gen Virol* 53: 343-346.
26. Sharma A, Mahinghara B, Singh A, Kulshrestha S, Raikhy G, et al. (2005) Identification, detection and frequency of lily viruses in northern India. *Scientia Horticultrae* 106: 213-227.
27. Liu Y, Wang R, Guo X, Dai J (2007) A cross-sectional TEM sample preparation method for films deposited on metallic substrates. *Materials characterization* 58: 666-669.
28. Lichtenthaler H (1968) Plastoglobuli and the fine structure of plastids. *Endeavour* 27: 144-149.
29. Austin JR, Frost E, Vidi PA, Kessler F, Staehelin LA (2006) Plastoglobules are lipoprotein subcompartments of the chloroplast that are permanently coupled to thylakoid membranes and contain biosynthetic enzymes. *The Plant Cell* 18: 1693-1703.
30. Martin E, Hine R (2015) *A dictionary of biology*. Oxford University Press, USA.
31. Whitton B, Peat A (1967) Heterocyst structure in *Chlorogloea fritschii*. *Archiv für Mikrobiologie* 58: 324-338.
32. Greenwood F, Hunter WM, Glover J (1963) The preparation of <sup>131</sup>I-labelled human growth hormone of high specific radioactivity. *Biochemical Journal* 89: 114.
33. Buléon A, Colonna P, Planchot V, Ball S (1998) Starch granules: structure and biosynthesis. *Int J Biol Macromol* 23: 85-112.
34. Martelli GP, Russo M, Rubino L (1973) Eggplant mottled dwarf virus. *CMI/AAB Descriptions of plant viruses* 115.

35. Martelli GP, Russo M (1977) Plant virus inclusion bodies. *Advances in virus research* 21: 175.
36. Roberts WL, Hammond DM, Speer CA (1970) Ultrastructural study of the intra-and extracellular sporozoites of eimeria callospermophili. *The Journal of parasitology* : 907-917.
37. Kim KS, Fulton J (1972) Fine structure of plant cells infected with bean pod mottle virus. *Virology* 49: 112-121.
38. Zitter TA, Murphy JF (2009) Cucumber mosaic. *The plant health instructor*.
39. Montasser M, Al-Sharidah A, Ali N, Nakhla M, Farag B, et al. (1999) A single dna of tomato yellow leaf curl geminivirus causing epidemics in the state of kuwait. *Kuwait J Sci Eng* 26: 127-141.
40. Montasser MS (1999) Experimental protocols in virology and immunology. Academic Publication Council, Kuwait University 1<sup>st</sup> issue, 166.
41. Abràmoff MD, Magalhães, PJ, RAM SJ (2004) Image processing with ImageJ *Biophotonics international* 11: 36-42.
42. Schneider CA, Rasband WS, Eliceiri KW (2012) NIH Image to ImageJ: 25 years of image analysis. *Nat methods* 9: 671-675.
43. Montasser MS (2012) US Patent No. 8,138,390 B2 : Biological control agent for plants.
44. Honda Y, Matsu C (1974) Electron microscopy of cucumber mosaic virus-infected tobacco leaves showing mosaic symptoms. *Phytopathology* 64: 534-539.
45. Raj S, Srivastava A, Chandra G, Singh B (2002) Characterization of *cucumber mosaic virus* isolate infecting gladiolus cultivars and comparative evaluation of serological and molecular methods for sensitive diagnosis. *Current science Bangalore* 83: 1132-1137.
46. Shintaku MH, Zhang L, Palukaitis P (1992) A single amino acid substitution in the coat protein of *Cucumber mosaic virus* induces chlorosis in tobacco. *The plant cell* 4: 751-757.
47. Pyke KA, Leech RM (1994) A genetic analysis of chloroplast division and expansion in *arabidopsis thaliana*. *Plant Physiol* 104: 201-207.

### Author Affiliations

[Top](#)

<sup>1</sup>Department of Biological Sciences, University of Kuwait, Kuwait

<sup>2</sup>Nanoscopy Science Center, University of Kuwait, Kuwait

### Submit your next manuscript and get advantages of SciTechnol submissions

- ❖ 80 Journals
- ❖ 21 Day rapid review process
- ❖ 3000 Editorial team
- ❖ 5 Million readers
- ❖ More than 5000 
- ❖ Quality and quick review processing through Editorial Manager System

Submit your next manuscript at • [www.scitechnol.com/submission](http://www.scitechnol.com/submission)